46th AIAA/ASME/SAE/ASEE Joint Propulsion Conference & Exhibit
25 - 28 July 2010, Nashville, TN

AIAA 2010-7047

HM7B Simulation with ESPSS Tool on Ariane 5 ESC-A Upper Stage

Armin Isselhorst, Propulsion Systems, TE59
EADS Astrium GmbH, P.O. Box 286156, 28361 Bremen, Germany

ESPSS tool project which was proposed, coordinated and funded by ESA is dedicated for launcher stage and space vehicle functional performance analysis. The main tool developer is EAI. The S/W development is concerned with setting up a common European platform for propulsion system simulation. Such a common platform is identified as crucial in order to strengthen the European company's competence in propulsion system modelling, which is important in case of a prime role responsibility or general industrial and research institute competence. ESPSS is proposed as a starting point and a framework for continuous cooperation on space propulsion systems between European industries working on such kind of systems. The paper will present for feasibility demonstration a gas generator engine cycle application using exemplarily A5 ESC-A HM7B engine. The set-up of the model is based on HM7B definition file and takes as a 1st approach the engine steady state conditions for adjustment of the main input parameter sets. The steady state conditions of H10-III engine were taken as reference. Part of the physical model formulation of its incorporated components, its schematic, data initialisation and simulation results obtained will be shown. The simulation results will be compared to respective flight measurement data of an A5 ESC-A upper stage.

Nomenclature

A	=	cross section
d	=	diameter
J	=	moment of inertia
m	=	mass flow rate
n	=	rotation number
η	=	efficiency
p	=	pressure
P	=	power
s	=	thickness
T	=	temperature
V	=	volume
π	=	pressure ratio
N	=	rotation velocity coefficient
φ^+	=	mass flow coefficient
Ψ^+	=	head rise coefficient
C^+	=	torque coefficient
λ^+	=	power coefficient

I. Introduction

ESPSS project was proposed by EAI and is dedicated for launcher stage and space vehicle functional performance analysis. The development is funded by ESA. The S/W development is concerned with setting up a common European platform for propulsion system simulation. Such a common platform is identified as crucial in order to strengthen the European company's competence in propulsion system modelling, which is important in case of a prime role responsibility or general industrial and research institute competence. ESPSS is proposed as a starting point and a framework for continuous cooperation on space propulsion systems between European industries working on such kind of systems.

ESPSS is based on the framework provided by EcosimPro kernel, a generic system simulation tool, originally developed for ECLSS Simulation for manned spacecraft. EcosimPro is a state-of-the-art tool capable of modelling any kind of dynamic system represented by DAE or ODE and discrete events. It is integrated in a visual environment similar to MS Visual Studio®. EcosimPro provides an object-oriented approach towards creating reusable component libraries for modular model building and is able to process and solve complex DAE systems. EcosimPro offers most of the functionality required by the ESPSS tool and minimum changes or upgrades will be required.

The objective of the ESPSS project was to physical model space propulsion system H/W components for the simulation of such kind of systems. The structure of the tool is flexible enough to model different kinds of space propulsion systems: chemical rocket propulsion, nuclear and solar electrical propulsion.

The paper will present for feasibility demonstration a gas generator engine cycle application using exemplarily ARIANE 5 ESC-A HM7B engine. The set-up of the model is based on HM7B definition file and takes as a 1st approach the engine steady state conditions for adjustment of the main input parameter sets. The steady state conditions of H10-III engine were taken as a reference. Part of the physical model formulation of its incorporated components, its schematic, data initialisation and simulation results obtained will be shown. The simulation results will be compared to respective flight measurement data of an ARIANE 5 upper stage ESC-A stage.

II. HM7B Engine

The bi-propellant and cryogenic upper stage ESC-A is the latest improvement of the ARIANE 5 and can be used instead of the EPS in case re-ignition is not needed. Being the 3rd and last stage ESC-A completes the mission by ejecting satellite into their specified orbit. It is the main contribution to the ability of lifting up to 9 t into GTO.

The ESC-A stage has a reference diameter of 5400 mm and a height of 4711.6 mm (outer covering). The 2 propellant tanks for liquid Hydrogen and liquid Oxygen have a volume of 39.4 m^3 and 11.4 m^3, respectively. The liquid Hydrogen (LH2) tank is operated at 2.8 to 3.0 bar, the liquid Oxygen (LOX) tank at 1.97 to 2.06 bar. A spherical helium vessel for the pressurization of the pneumatic control system and the LOX tank is located at the bottom of the BMA carrying 172 l of GHe at 226 bar and 85 K.

The ESC-A is propelled by the HM7B motor which was already developed for ARIANE 1 3rd stage and successfully flown on ARIANE 1 to 4 launchers. A photo and a simplified sketch are shown below:

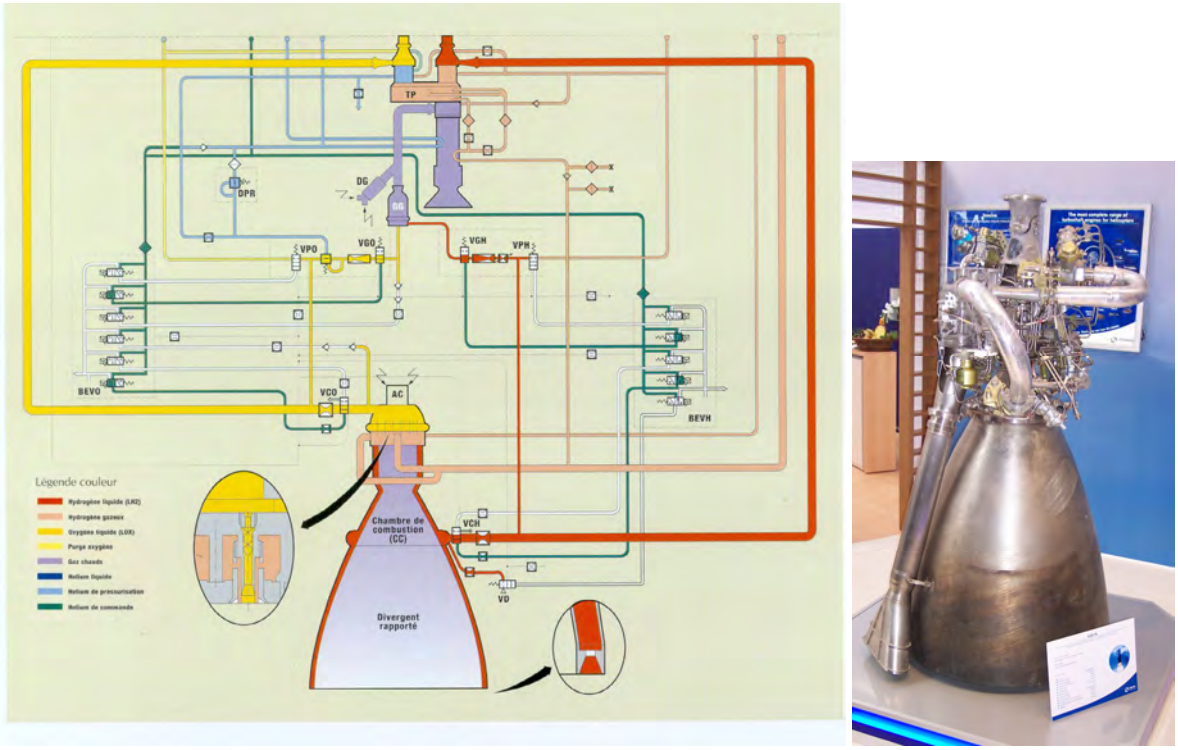

Figure II-1. HM7B engine

In order to ensure numerical correct behaviour and the right interpretation of results due to the change of parameters the correlation of the whole model is subdivided into 3 steps:

1. Correlation of the turbo-pump
   This 1st step makes sure that the turbo-pump gives the right results. This is an important prerequisite, because a wrong adjusted turbine would result in deviating pressure heads, temperatures, rotation speeds and propellant mass flow rates. Therefore, the turbo-pump has to be verified before the simulation study of the entire system.
2. Correlation of combustion chamber
   The next step includes the verification of the combustion chamber which of course influences the entire system in terms of mass flow and pressures in the same way as the turbo-pump does.
3. Correlation of the entire system including piping system
   The true correlation of the entire system is performed as a last step. Knowing that a given turbo-pump characteristic results in a correct thrust, mixture ratio, mass flows and chamber pressure of the combustion chamber makes it possible to determine the right pressure losses in the piping system by the given steady state values.

A. Turbo-Pump Correlation

The 1st part of the correlation covers the turbo-pump. With a fairly simple model the turbine incl. pumps, gear box and exhaust nozzle can be adjusted to the steady state values. Because each pump has a given pressure head for a given mass flow rate an adjusted orifice can be used with the same behaviour but vice versa w.r.t. Δp.

Figure II–2 shows the schematic of the turbo-pump. It includes also the gaseous Helium flushing at start-up of the gas generator.

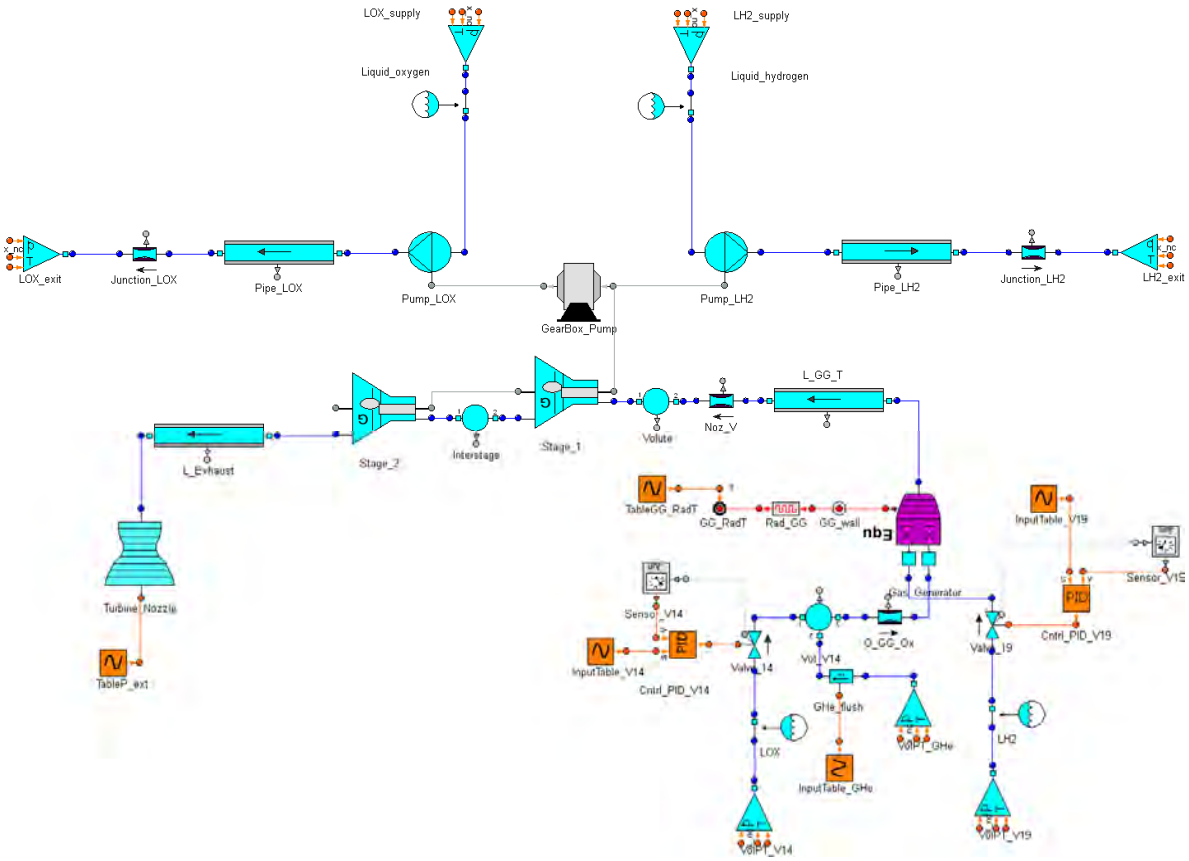

Figure II-2. ESPSS Schematic [9] Representation of Turbo-Pump

The pump characteristics are taken from turbo-pump internal documentation. The relevant parameters are:

- mass flow coefficient: $\varphi^+ = \frac{\dot{m}}{\rho\omega}$
- head rise coefficient: $\Psi^+ = \frac{\Delta p}{\rho\omega^2}$
- torque coefficient: $C^+ = \frac{M}{\rho\omega^2}$
- power coefficient: $\lambda^+ = \frac{C^+}{\varphi^+} = \frac{P}{\dot{m}\omega^2}$

The default pump model curves for head rise and torque coefficient were adjusted with the steady state pump parameters, accordingly.

The turbine characteristics are taken from the turbo-pump internal documentation. The turbine characteristics are derived from iterative adoption of simulations to obtain the correct pressures and temperatures, rotation velocity and power of the turbine. The relevant definitions are:

- rotation velocity coefficient: $N = \frac{r \cdot \omega}{c}$
- pressure ratio: $\pi = \frac{p_i}{p_o}$

The gas generator characteristics and geometrical data are taken from the turbo-pump internal documentation.

Additional parameters are the injector loss coefficients, which are set by EAI default to $\varsigma = 2$, without possibility of modification. Adoption of the pressure loss between head and chamber is actually only possible by injector cross section variation. The nozzle is defined via normalized nozzle diameter d_{noz}/d_{th} versus non-dimensional axial position.

The expansion nozzle characteristics are derived from iterative adoption of simulations to obtain the correct turbine outlet pressure from the turbo-pump internal documentation. Additional parameters are the nozzle length and the throat diameter.

Table II–1 shows the deviation between nominal pump data and model results:

pump	ΔP [%]	Δn [%]	$\Delta\dot{m}$ [%]	Δp_{out} [%]
LOX	+ 14.1	+ 0.36	+ 0.25	+ 0.5
LH2	- 2.9	+ 0.36	± 0	- 0.2

Table II-1. Model Accuracy of Pumps

The accuracy of adjustment could be well performed with the used pump models for steady state characterisation. It can be seen that the deviation of the power is relatively high which implies that the adjustment of the text book curves w.r.t. torque coefficients of the pumps can be improved still further. However, the sum of driving power has only a little deviation of 0.1 %.

The turbine mass flow rate and the mixture ratio are adjusted via 2 PID controllers on the 2 gas generator feeding valves, so that deviations amount to ~0%. The total turbine power has a deviation of + 0.6%.

From Table II–2 it is remarkable that maximum deviation occurs on the inter-stage pressure of ~ 11.1%. Generally, the deviations can be further reduced by more iterative adjustment loops.

Table II–2 shows the deviation between nominal power unit data and model results:

power unit	Δp [%]	ΔT [%]
gas generator	- 1.3	+ 2.0
volute	+ 1.3	+ 4.4
1st stage interstage 2nd stage	- 11.1	
exhaust pipe	- 3.6	+ 8.4

Table II-2. Model Accuracy of Power Unit

The thrust of the model nozzle deviates -8.7%.

B. Thrust Chamber Correlation

The 2nd part of the correlation covers the combustion chamber. With a fairly simple set of parameters the thrust chamber can be adjusted to the steady state values, because at relevant chamber positions pressures, temperatures and mass flows are known. Additionally, the chamber contour is possible to define.

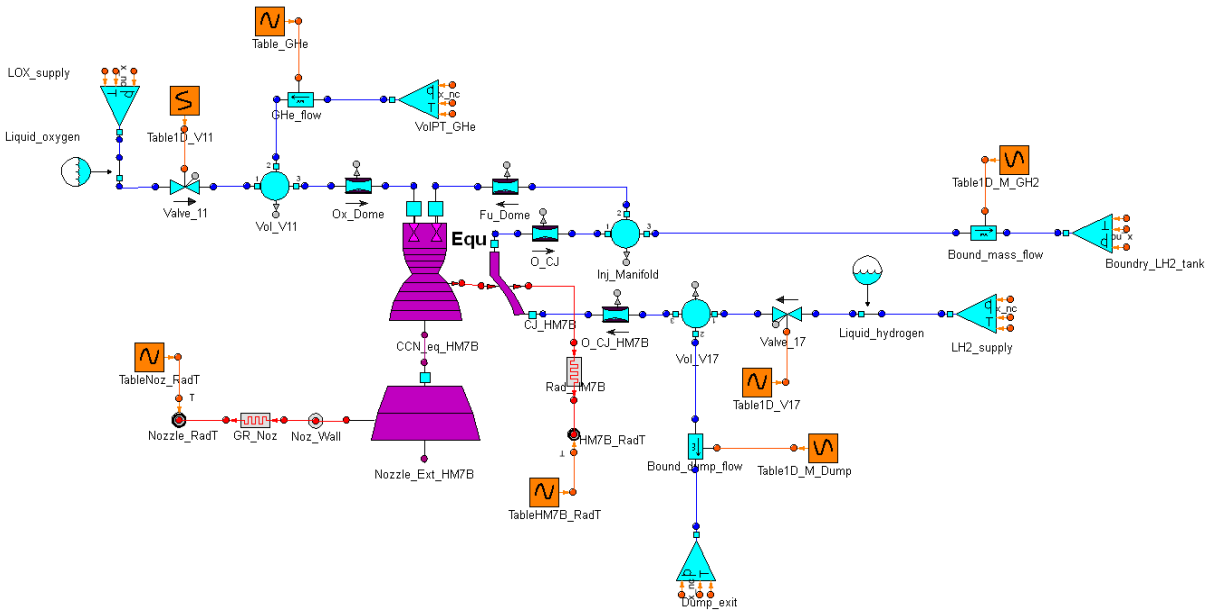

Figure II-3. ESPSS Schematic [9] Representation of Thrust Chamber

Figure II–3 shows the schematic of the thrust chamber. The relevant steady state thrust chamber data are taken from the thrust chamber internal documentation. It includes also the gaseous Helium flushing on Ox-dome side at start-up and shut-down. The tap-of mass flow at injector manifold ring is also considered for continuous LH2 tank pressurization. The geometry of the cooling jacket is included in detail as well as the expansion nozzle geometry via defining the normalized nozzle diameter d_{noz}/d_{th} versus non-dimensional axial position.

The combustion chamber incl. convergent nozzle part is used to normalize the related axial position. The divergent supersonic nozzle length is used to normalize the related axial position. The nozzle efficiency is set to 0.97. The dump cooling cannot be considered due to lack of COMPONENT. A nozzle throat discharge coefficient c_d of 0.98 is considered via reduction of the geometrical throat diameter. The LOX/LH2 injectors are characterized by by their total cross section and the related volumes.

The injector heat capacity is estimated to a global value of 5000 W/K and the chamber to injector head conductance is set to 400 W/K. There is actually no distinction possible between convective and radiation heat transfer nor a possibility to consider that the Ox-dome is thermally in series to the Fu-dome.

thrust chamber	Δp [%]	ΔT [%]	$\Delta \dot{m}$ [%]
LOX Dome	0.2	0	0.08
LH2 Dome	- 0.65	- 15.7	0.14
LH2 RC_{in}	0	1	- 0.12
CC	- 0.08		- 0.07
Dump			0

Table II-3. Model Accuracy of Thrust Chamber

From Table II–3 it is remarkable that maximum deviation occurs on the cooling jacket outlet temperature of ~15.7%. Here, the heat transfer model between combusted gas and chamber wall must be enhanced and/or the heat transfer model for the channel flow. Higher space discretization has not led to an improved result.

C. HM7B Engine Correlation

The ESPSS engine model, Figure II–4, is set-up according the HM7B motor. It has been reduced to the main functional components to characterize and adjust the behaviour and performance of the motor for the standard H10-III and ESCA steady state phase taken from internal documentation.

The engine is composed of the following main components:

- 2 propellant feed lines incl. tank outlet valves
- 1 gas generator
- 2 pyro igniters
- 2-stage turbine with heater incl. expansion nozzle
- 2 single stage radial pumps
- 1 gear box incl. ventilation system
- lubricant system
- 2 gas generator injector blocks
- 2 engine valves
- 1 regenerative cooled combustion chamber incl. gaseous hydrogen tap-of
- 1 dump-cooled supersonic nozzle extension
- entire piping system

Simplifications are introduced by not considering the pressurization gas circuit for the pilot valves. The main engine valves and the propellant feed line valves are controlled by a time-dependent data table. The gas generator injection blocks for LOX and LH2 are simplified to PID controlled valves with a regulated flow rate each introduced as a set value. The Helium heating circuit is also not considered as well as the gaseous Helium and Hydrogen flushing of the gear box and its lubrication. The dump cooling flow of the supersonic nozzle extension is only considered as wasted flow by a respective adjusted mass flow rate. With these simplifications the HM7B schematic was built.

The 3rd part of the correlation covers the whole engine system. With the discussed set of pre-adjusted parameters the engine model is now capable to obtain the steady state values. Unknown values e.g. pressure losses in the lines are thereby easy to determine. A comparison is further made to transient flight measurement transducers although a realistic transient simulation needs a certain number of volumes per pipe section.

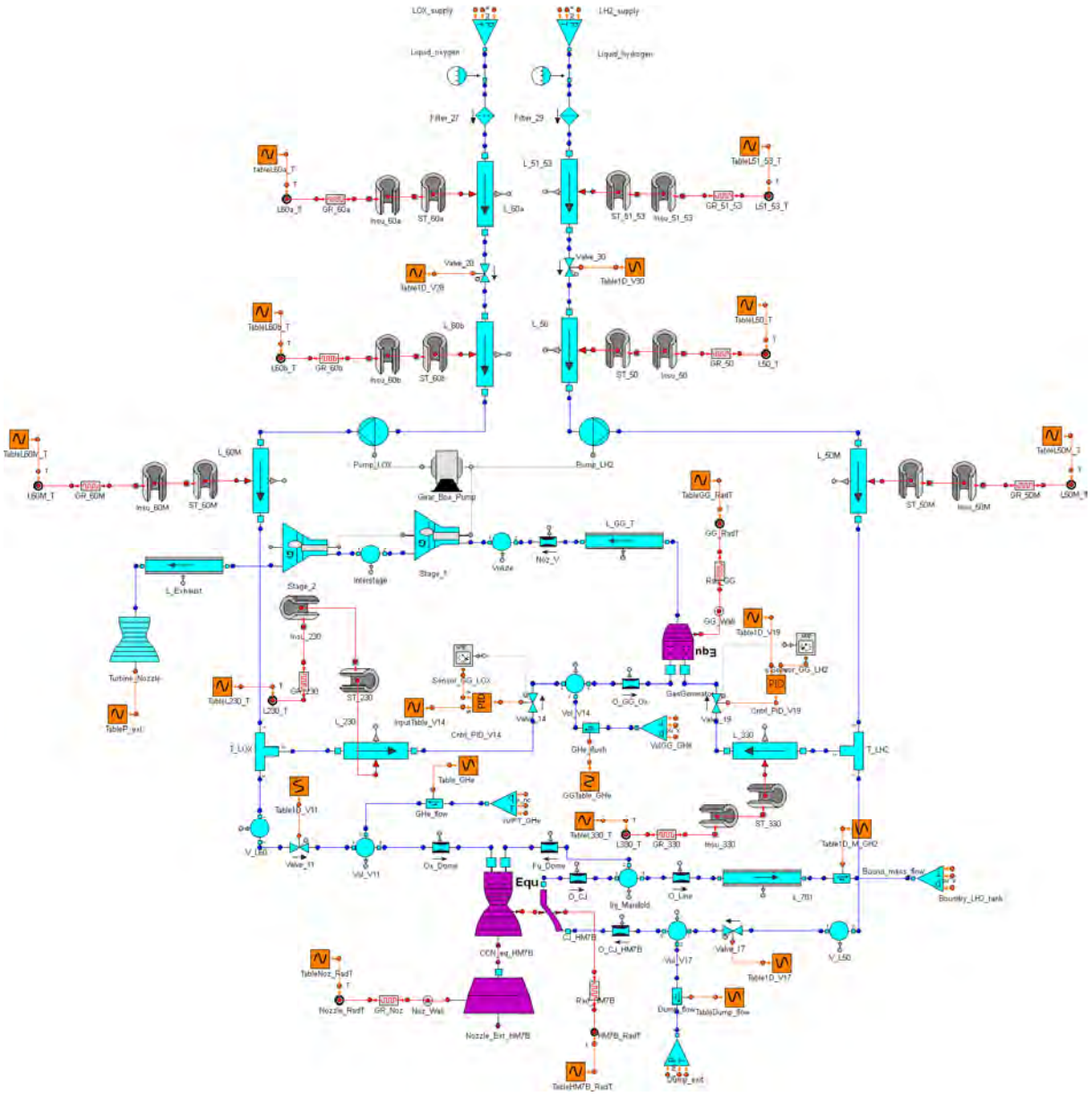

Figure II-4. ESPSS Schematic [9] Representation of HM7B Engine

The LOX/LH2 injector blocks for the gas generator are highly simplified w.r.t. the real functional H/W design. As the mass flow is controlled to the specified values no data are essentially necessary to include to the model.

The obtained thrust by the full model differs only by ~70 N.

A remarkable deviation from the full engine model on the CC is the lower pressure at inlet of LH2 Chamber valve of ~0.7 bar coming from the lower LH2 pump outlet pressure of the pump. It is a result of the lower pump rotation of ~ 360 U/min. Additional, there is another 0.5 bar which will results from the lower valve inlet temperature of 0.8 K. The globally 1 K lower averaged temperature in the RC circuit result in a 50% lower pressure loss, so that finally the pressure at the RC outlet is in both models the same. Whether this can be realistic has to be further checked.

The observed deviation in Ox-dome pressure can be explained by the lower pump rotation of ~ 77 U/min.

Although the turbine mass flow rate and the mixture ratio are well adjusted via the 2 PID controllers on the 2 gas generator feeding valves, the deviation in gas generator pressure amounts to -0.7 bar which is responsible for the lower turbine power of 7.1 kW. The total turbine power is ~400 kW. An explanation can only be the slight difference in LH2 inlet temperature of ~0.7K.

III. HM7B Flight Data Correlation

In the final part of the correlation the HM7B model is compared to flight data measurements of A5 L521. Flight measurements serve as the basis for the evaluation of the computed values. Since the present correlation is focused on the engine the regarded sensors include the LH2/LOX system pressure sensors as well as the temperature sensors. Additionally, 2 revolution sensors are used as well as the 2 delta-p sensors.

A. Engine Start-Up Correlation

Figure III–1 shows the thrust chamber pressure evolution during start-up inside the thrust chamber. In the simulation the pressure increase starts slightly later compared to the measurement, which seems to be a result of the chosen LOX chamber valve time constant of 0.01s. The pressure increase follows now good the measurement. The still existing slight differences can be further reduced by on-going parameter adjustment. Now, the gas generator chamber pressure is during pyro-starter operation in good equivalence to the respective measurement, see Figure III–2. The slight decrease of starter pressure evolution is related to decrease in mass flow rate and could be adapted by defining a time-dependent mass flow rate in the model. A slight over-oscillation can be still remarked.

This "over-oscillation" is clearly an effect of the pumps outlet pressures see Figures III–3 and III–4. When changing from pyro-starter operation mode to LH2/LOX combustion mode, it can be remarked that the simulated pressure curves increase faster. This can also be observed on the rotation speed of the turbine axle, see Figure III–5. The slope of the gas generator pressure increase is in the 1st phase identical to the measurement, but from a certain time onwards (~536.75s) it over-shoots the measured pressure. This seems to be a result of the simplified injector block valves for LOX/LH2. A better adjustment of the PID parameters may reduce this over-shooting effect coming from a higher mass injection at this event compared to the H/W case.

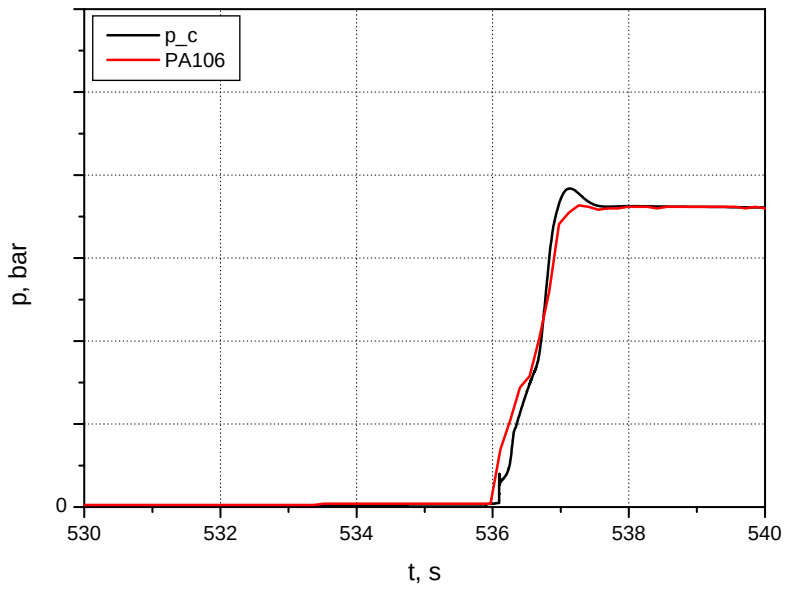

Figure III-1. Thrust Chamber Pressure p_c: Sim. / Meas.

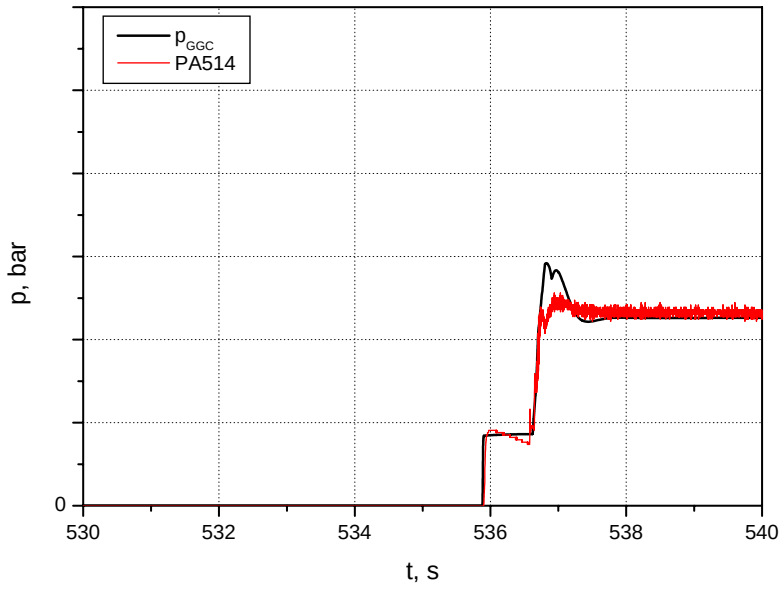

Figure III-2. Gas Generator Chamber Pressure p_c: Sim. / Meas.

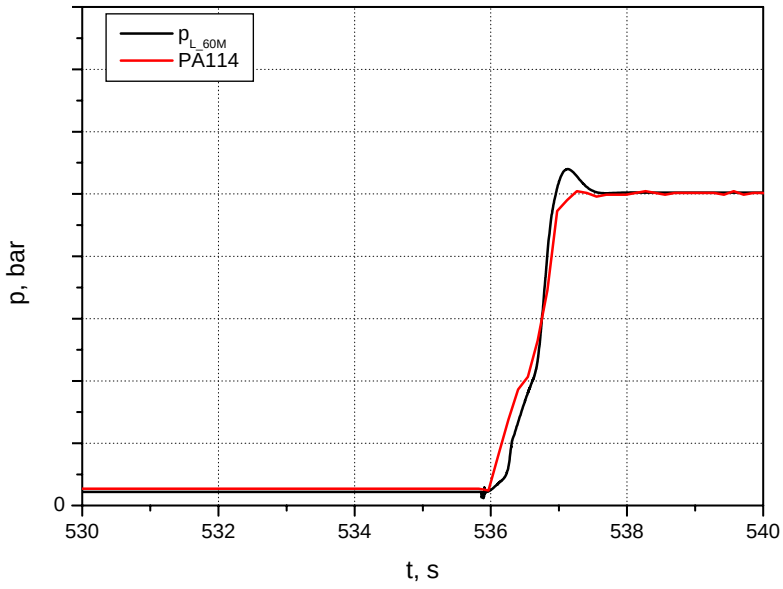

Figure III-3. Downstream LOX Pump Pressure p_{L_60M}: Sim. / Meas.

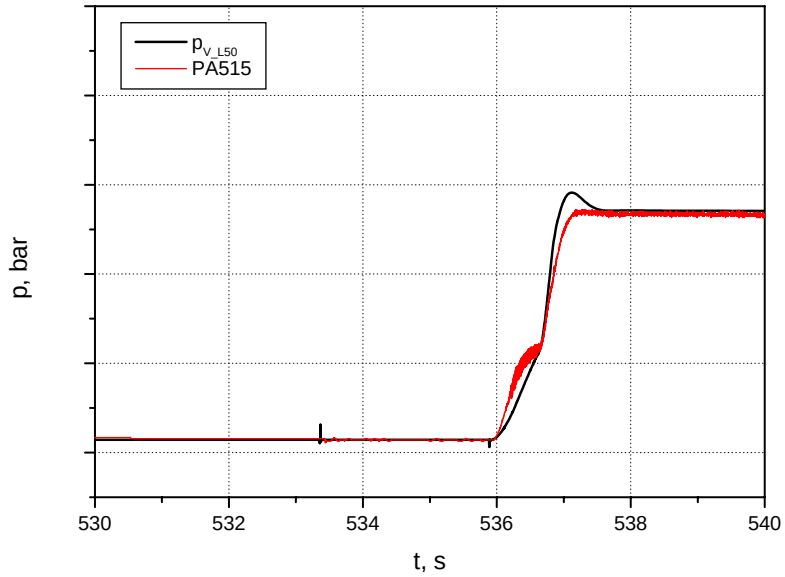

Figure III-4. Downstream LH2 Pump Pressure p_{V_50}: Sim. / Meas.

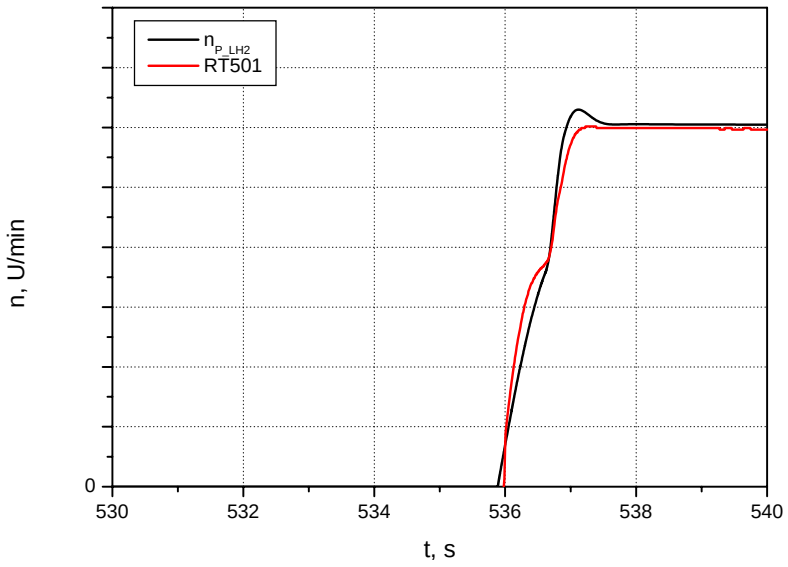

Figure III-5. LH2 Pump Rotation number n: Sim. / Meas.

Figure III–6 shows the turbine exhaust pipe temperature which increases very steep up to ~ 1180 K. This cannot be observed in the respective temperature measurement. The clear reason here is the non-consideration of the thermal mass of the turbine housing and stator and rotor in the turbine model. Here, the heat will be stored by heating up the mass to the working thermal conditions. Actually, there is no possibility to respect for this in ESPSS model. A further effect will be the transducer's limited rise-response time constant.

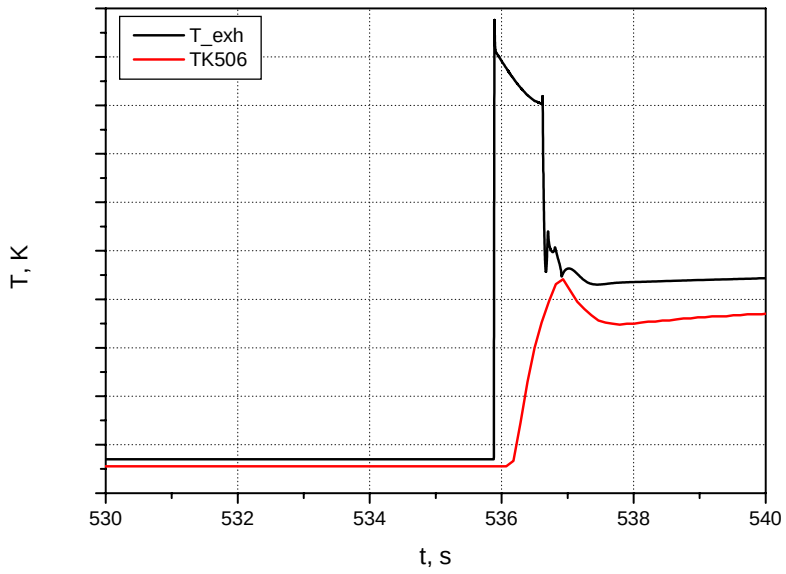

Figure III-6. Turbine Exhaust Pipe Temperature T_{exh}: Sim. / Meas.

B. Engine Steady-State Correlation

The next simulation case presents the comparison of the flight sequence between 500 and 1500 s related to H0. It includes the *3-times lower* chosen start-up gas generator chamber pressure by reducing the *pyro-starter mass flow rate* of a factor of 3.

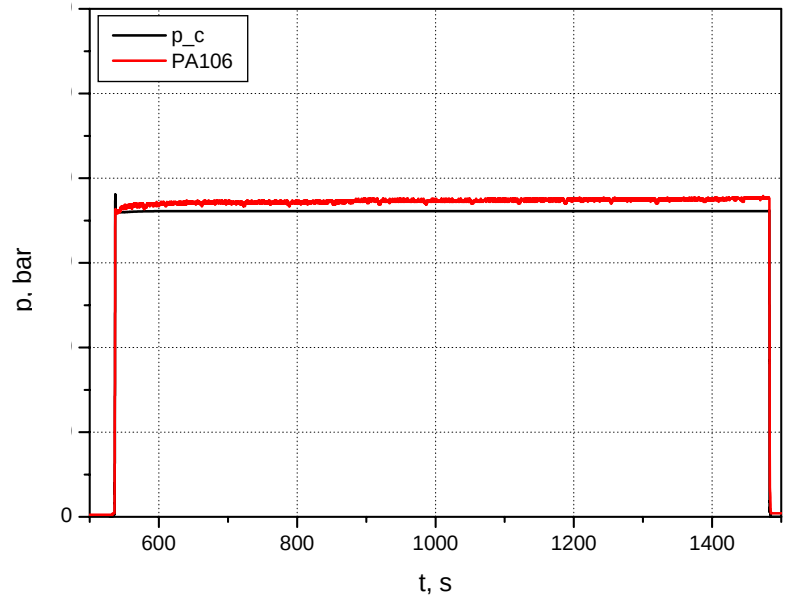

Figure III-7. Thrust Chamber Pressure p_c: Sim. / Meas.

The measured thrust chamber pressure is ~1.2 bar higher in flight compared to the simulation, see Figure III–7. For the steady state adjustment of the engine model the H10-III data were used, because here all data for turbo-pump are available. On ESC-A stage the operation point of the motor is slightly deviated.

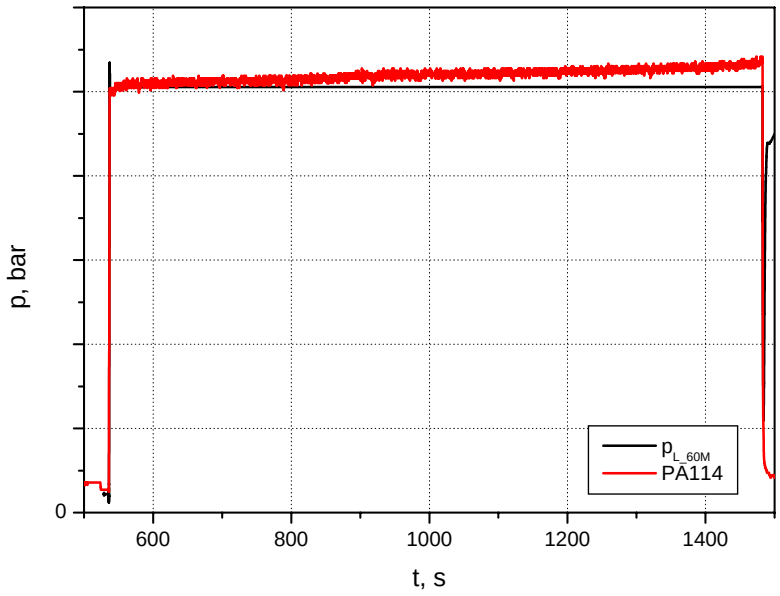

Figure III-8. Downstream LOX Pump Pressure p_{L_60M}: Sim. / Meas.

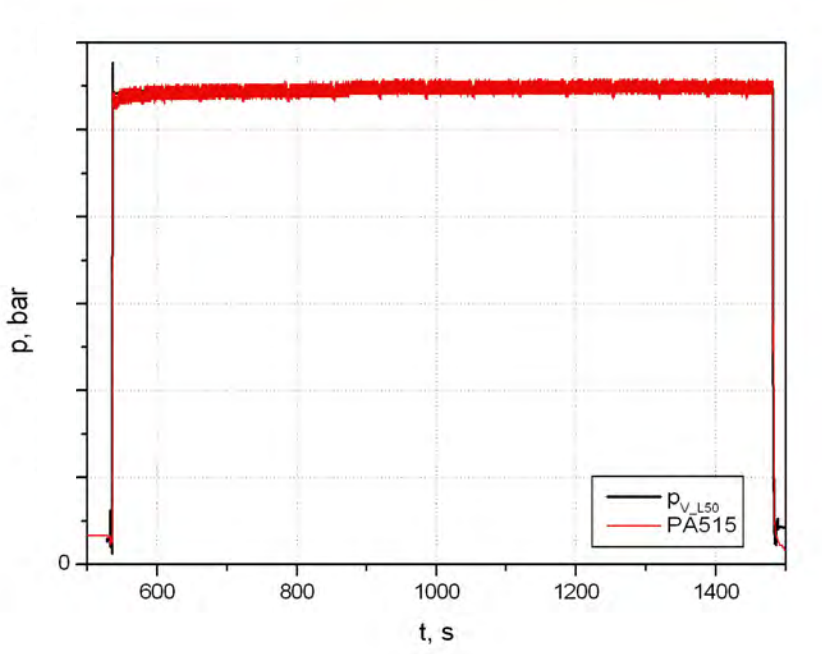

Figure III-9. Downstream LH2 Pump Pressure p_{V_50}: Sim. / Meas.

Figure III–8 and III–9 show the downstream LOX and LH2 pump pressure, respectively. While LH2 pump outlet pressure increases only 1.2 bar and fits therefore good to the simulated curve, the LOX pump outlet pressure increases of ~ 3 bar which is not observed on the simulated curve. According to Figure III–10, the turbine rotation speed increases slightly in flight from about 60,000 to 61,500 U/min at end of thrust phase. This rotation speed increase explains well the pressure increases; the effect on LOX is higher, because of the higher efficiency on LOX side, with nearly no temperature increase of fluid while LH2 increases during thrust phase of 1.5 K with a strong impact on the density.

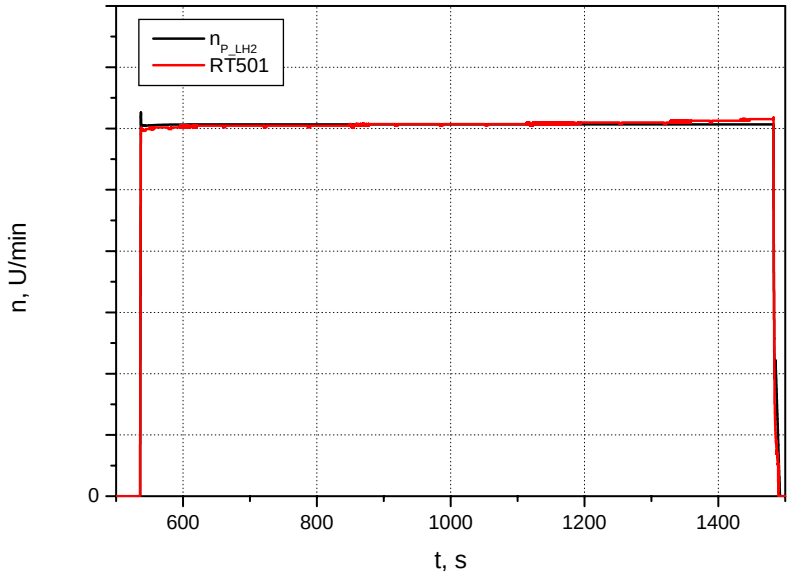

Figure III-10. LH2 Pump Rotation Number n: Sim. / Meas.

IV. Conclusion

This paper presents the cryogenic engine model for industrial evaluation in frame of ESPSS using a gas generator cycle engine application. Exemplarily, the HM7B engine of A5 ESC-A was chosen. The set-up of the model is based on HM7B internal documentation and accessible technical drawings and takes thereby as a 1st approach the engine steady state conditions for adjustment of the main input parameter sets for the model. The steady state of H10-III engine was taken as a reference. A good achievement of the steady state conditions could be obtained with the help of an iterative process of parameter adjustments and 2 sub-models. The axial discretization of all pipe components was set to *one*, because actually, hydraulic wave effects were not of interest. After the ESC-A SCAR phase correlation of L522 it can be concluded that even though the tank model with settled propellant is a crucial simplification with respect to the phase interface contact area between liquid and ullage coupled with liquid sloshing which results in additionally transferred heat, it still delivers very realistic results.

A comparison to ESC-A conditions which incorporates also a comparison to ESC-A flight transducer data has been performed. The obtained results show that principally a good agreement to transducer data could be achieved with the steady state adjustment. The only necessary post-adjustment was the reduction of the gas generator pyro-starter mass flow rate to correct the combustion pressure during the starting phase. This has to be considered, because in the model the pyro-starter is inside the gas generator component.

Simulation speed of the model is acceptable for engine start-up which is in the order of 4 to 10 min. Full flight missions have taken 40 min. This long simulation is mainly affected by the long time shut-off simulation event.

For further work in the future, following recommendations for improvements can be proposed:

- to include the thermal mass incl. heat transfer of the turbine wheels, shaft and housing into the turbine model formulation

- to set-up a separate pyro-starter model for turbine start
- to improve the regenerative cooling jacket heat transfer model formulation

Acknowledgments

The ESPSS project Part I (physical formulations and software development) and II (software feasibility demonstration) were funded by ESA (European Space Agency) with Contract No. 21490/08/NL/CP and were performed at EAI Madrid, Spain, CENAERO, Belgium and Astrium GmbH Bremen, Germany.

References

Reports, Theses, and Individual Papers

[1]Isselhorst, A.; *Simulation of Launcher Propulsion Systems, Study on numerical Modeling and Simulation of Launcher Stages for propelled and non-propelled Flight Phases*, Final Report Part I 2006, BMBF account no. 50JR0503.

Astrium GmbH Internal Documents

[2]Isselhorst, A.; *Mathematical Model Formulations for Propellant Tanks*, Astrium GmbH, Germany, ESPSS-RIBRE-TN-0001, 31.01.2007

[3]Lux, J.; *Solid Property Functions*, ESPSS-RIBRE-TN-0002, Astrium GmbH, Germany, 19.12.2006

[4]Isselhorst, A.; *Mathematical Model Formulations for Pneumatic and Hydraulic Pipes*, Astrium GmbH, Germany, ESPSS-RIBRE-TN-0003, 28.02.2007

[5]Lux, J.; *EcosimPro interface to the FORTRAN surface shape routines*, Astrium GmbH, Germany, ESPSS-RIBRE-TN-0004, 31.01.2007

[6]Lux, J., Isselhorst, A.; *FUNCTIONS for Propellant Tank Geometries*, Astrium GmbH, Germany, ESPSS-RIBRE-TN-0007, 31.01.2007

[7]Wagner, T.; *Mathematical Model Formulations for Engine Injector Head, Combustion Chamber, convergent-divergent Nozzle and Cooling Jacket*, Astrium GmbH, Germany, ESPSS-RIBRE-TN-0010, 28.02.2007

[8]Lux, J.; Isselhorst, A.; *Physical Formulation of Control Elements for Pneumatic Pipe Networks*, Astrium GmbH, Germany, ESPSS-RIBRE-TN-0006, 28.02.2007

[9]Isselhorst, A.; *HM7B Engine Model with ESPSS*, Astrium GmbH, Germany, ESPSS-RIBRE-TN-0012, 28.02.2009

Computer Software

[10]EA International, Madrid, 2008, *User Manual EcosimPro v4.4*

[11]EA International, Madrid, 2009, *ESPSS Libraries User Manual, Iss 1*

[12]EA International, Madrid, 2008, *SOW of EADS Contribution to ESPSS Part 2*

[13]EcosimPro; *A Professional Dynamic Modeling and Simulation Tool for Industrial Applications*, v4.4, EAI **E**mpresarios **A**grupados **I**nternational, Madrid, Spain, 2009.